Journal of Nuclear Materials 560 (2022) 153504

Contents lists available at ScienceDirect

Journal of Nuclear Materials

journal homepage: www.elsevier.com/locate/jnucmat

Monitoring the gradual change in oxidation state during surface oxidation or reduction of uranium oxides by photoemission spectroscopy of the 5f states

Ghada El Jamal[a], Thomas Gouder[b,*], Rachel Eloirdi[b], Mats Jonsson[a]

[a] KTH, School of Engineering Sciences in Chemistry, Biotechnology and Health (CBH), Department of Chemistry, Applied Physical Chemistry
[b] European Commission, Joint Research Centre (JRC), Karlsruhe, Germany

ARTICLE INFO

Article history:
Received 6 July 2021
Revised 10 December 2021
Accepted 29 December 2021
Available online 31 December 2021

Keywords:
UO_2
Oxidation
Reduction
XPS-UPS
Atomic oxygen- hydrogen
Quantification methods

ABSTRACT

Photoelectron spectroscopy study of the U5f emission gives valuable insight into the surface oxidation mechanism of uranium oxides. Its intensity is directly related to the electron count n_f, which decreases with increasing oxidation number (U(IV): n_f=2; U(V): n_f=1; U(VI): n_f=0). n_{5f} can be quantified by analysing the U5f/U4f intensity ratio and using a standard of known composition. In addition, the 5f emission has a characteristic multiplet shape, directly related to n_{5f}, which can be used to distinguish the $5f^2$ and $5f^1$ configuration of U(IV) and U(V), respectively. Three independent methods are used to determine the surface oxidation state: the U5f/U4f intensity ratio, the relative intensities of the U4f oxide shifted peaks, and the O1s/U4f intensity ratio. The first two reveal the concentration of the U in each oxide, the third indicates the total concentration of oxygen. These methods are applied to follow the surface modification of UO_2 films when exposed to various oxidative conditions: molecular and atomic oxygen and water plasma at 400°C. In addition, the reduction of UO_3 by atomic H is studied. Molecular oxygen oxidizes UO_2 to UO_{2+x}(x = 0.22), containing both U(IV) and U(V). Atomic oxygen also oxidizes U(IV) to U(V) at low dosages, but then continues oxidizing U(V) to U(VI) (UO_3) at high dosages. Conversely, atomic hydrogen reduces UO_3. In the early phase of reduction U(V) forms exclusively – no U(IV) is observed. Water plasma first transforms almost all UO_2 (surface and subsurface) into U(V). With further plasma exposure the surface is oxidized to about 80% U(VI) and 20% U(V). Up to this point, a small fraction of U(IV) remains at the surface. Once it disappears, the surface oxidation stops and further water plasma exposure now leads to surface reduction into U(V) (the $5f^1$ peak increases again). Despite the reduction at high dosage, the O1s/U4f intensity ratio keeps increasing.

1. Introduction

Understanding the oxidation mechanism of UO_2 is of great importance for the assessment of the long-term stability of spent nuclear fuel exposed to groundwater in a failed geological repository. A scenario that has to be considered in the safety assessment of a geological repository for spent nuclear fuel is multiple barrier failure leading to groundwater intrusion. Should the fuel matrix (UO_2) dissolve it will release the contained long-lived radionuclides (e.g., Np, Pu, Am) into the environment. UO_2 itself has low solubility and would in general be stable in contact with water, in particular under the reducing conditions that prevail in many potential repository sites [1]. However, upon oxidation, e.g., by radiolytic oxidants produced in the groundwater in contact with the spent nuclear fuel, the solubility sharply increases. In general, the increased solubility is attributed to the formation of U(VI). Several studies have reported that uranium oxide starts to dissolve at stoichiometries from $UO_{2.33}$ and above [2]. It should be kept in mind that the dissolution of UO_2 also depends on the presence of potential complexing agents such as HCO_3^-/CO_3^{2-} and it has been demonstrated that the rate of dissolution depends on the concentration of these complexing agents as well as on the oxidant concentration [3,4]. The latter depends on the dose rate. There have been many studies on the surface oxidation of UO_2, its acceleration, and its inhibition [2,5,6].

Oxidation of nuclear fuel is an interfacial reaction occurring at the top surface of the fuel, which is in direct contact with the locally oxidizing environment. Surface spectroscopies have played a great role in its investigation. It is generally thought that oxy-

* Corresponding author.
E-mail address: thomas.gouder@ec.europa.eu (T. Gouder).

https://doi.org/10.1016/j.jnucmat.2021.153504

gen uptake first transforms $UO_{2.0}$ into $UO_{2.x}$ (x<0.33) which keeps the fluorite structure of UO_2. Local formation of U(V) must occur (at those U sites where there is additional oxygen bonding) but this does not seem to increase the solubility. U(V) can be observed on UO_2 surfaces exposed to radiolytic oxidants in aqueous solutions without added HCO_3^-, i.e., under conditions where dissolution of oxidized UO_2 is not favored [2]. In systems where HCO_3^- has been added, U(V) is in general not detected on the UO_2 surface after exposure to radiolytic oxidants. Formally a pure U(V) surface could be formed, for $UO_{2.5}$ (U_2O_5), but in general corrosion occurs through the formation of mixed valence oxides: U_4O_9 ($UO_{2.25}$ containing U(IV), U(V)), U_3O_7 ($UO_{2.33}$ containing U(IV), U(V)), U_3O_8($UO_{2.66}$ containing U(IV), U(VI) or U(V)/U(VI)) [7]. The U oxidation state determines the solubility of the oxides and an oxidant may very quickly generate the U(VI) oxidation state or it may rather generate first U(V) which is less soluble. However, previous studies of oxidative dissolution of UO_2 in aqueous systems have indicated that the rate limiting step is the first one-electron transfer step, i.e., from U(IV) to U(V) [5].

Determination of the actual oxidation state of U surface atoms is thus very important. In the literature the U4f core levels are most commonly used for this [8]. Their binding energies and their satellite structures are characteristic for individual oxidation states. Because of their specificity to uranium, they can also be used in complex materials containing other elements (as bulk components or surface impurities).

Another spectroscopic evidence of UO_2 surface oxidation comes from the U5f/O2p ratio, which has been used to follow UO_2 surface oxidation. The ratio was shown to decrease when UO_2 is oxidized to UO_{2+x}, which is due both to the decrease of the U5f and the increase of the O2p intensity [9]. In the present paper we also follow the evolution of 5f lines with oxidation.

Both intensity and shape of the 5f signal are related to the 5f occupancy (see below), which in turn depends on the oxidation state. By using an internal intensity reference, the U4f core level, the 5f count (n_{5f}) can be obtained (3.1.2). We show that the shape of the 5f emission also depends on the 5f count and provides a quite simple and straightforward way to deduce the oxidation state of uranium (U(V) and U(IV)) from the corresponding $5f^1$ and $5f^2$ electron configurations (3.1.3). These integer 5f occupations are the nominal occupations and neglect the covalent mixing of the U(5f) and O levels.

The results will be compared to the U4f analysis, which also provides the uranium oxidation state, by their characteristic U4f binding energies and the U4f satellites. Finally, the O1s/U4f intensity ratio gives information on the total oxygen concentration, without revealing how oxygen binds to uranium (for a given oxygen concentration, different distributions of oxidation states are possible).

In this work we compare the different methods mentioned above in monitoring the gradual change in oxidation state during surface oxidation or reduction of uranium oxides upon exposure to molecular and atomic oxygen, water plasma and atomic hydrogen. Some of these exposure cases have been previously published but are included in this context to enable a more complete comparison of the methods as well as the exposure scenarios.

The methods based on U-5f analysis only work in simple, pure and homogeneous oxides, where the U-5f states can be observed without interference from photoemission lines of other elements. Care is taken to prepare homogeneous surface films, by keeping the uranium layer thin (20 nm) and preparing the oxides at elevated temperature (typically 300 °C) where diffusion of oxygen, water and hydrogen is fast and concentration gradients are avoided. This study is not meant to replace the conventional U-4f speciation method but to show that it indeed correlates very well with the oxidation state, as observed by the U-5f states in binary oxides.

2. Experimental

2.1. Sample preparation

Uranium oxide films were prepared in-*situ* by direct current (DC) sputtering from a uranium metal target in a gas mixture of Ar (6 N) and O_2 (5 N), at partial pressures 5×10^{-3} mbar and 1×10^{-6} mbar, respectively. Deposition time and rate were chosen to prepare 20 nm thick $UO_{2.0}$ films. The uranium target voltage was fixed at −700 V. The plasma in the diode source was maintained by injection of electrons of 25–50 eV energy (triode setup), allowing working at low Ar pressure in the absence of stabilizing magnetic fields. The deposition was done on a polycrystalline Au foil substrate heated to 250 °C. Gold has been chosen because it is a metal, avoiding surface charging during photoemission, has a high melting point (1337 K), and is chemically inert, making sure oxidizing and reducing agents only react with uranium and not with the substrate.

2.2. Plasma source

The electrons were excited by an ECR (Electron Cyclotron Resonance) discharge based on stochastic heating of electrons by microwave radiation with permanent magnets. When the resonance condition between the electrons and the microwave electric field is fulfilled, the electrons gain sufficient energy to ionize the gas and sustain the plasma. In addition, they produce excited species, free radicals, and ions providing a reactive plasma environment. More details about the ECR source and different gas plasma characterization can be found in a previous study [10]. The wall of the plasma source consists in an alumina crucible, which is chemical inert and allows production of highly reactive plasma. O_2 and H_2 gas are used to generate atomic oxygen and hydrogen, respectively. The water plasma contains a complex mixture of oxidizing and reducing species (H, O, OH, H_2, O_2). In our experiment, the sample is placed in front of the source and exposed to the reactive species. A Pyrolytic Boron Nitride (PBN) heater installed below the sample holder maintained the sample temperature at 400 °C during the exposure to the plasma.

2.3. Surface characterization

High-resolution X-ray photoelectron spectroscopy experiments were performed using the Specs Phoibos 150 hemispherical analyzer and Al-Kα (1486.6 eV) excitation, produced by a XRC-1000 μ-focus source, equipped with a monochromator and operating at 120 W. The background pressure in the analysis chamber was 2×10^{-10} mbar. The spectrometer was calibrated using the $Au4f_{7/2}$ line of Au metal (83.9 eV BE) and the $Cu\text{-}2p_{3/2}$ line of Cu metal (932.7 eV BE).

3. Results and discussion

3.1. Separating the U5f and the valence band emissions in u oxides

Photoelectron spectra of the valence region (from 14 eV binding energy up to the Fermi-level) of uranium oxides contain the spectral lines of oxygen (O-2p) and uranium states (U5f,6d,7 s) (Fig. 1). The O-2p states form the valence band in the range from 3 - 10 eV, which, in addition, contains an admixture of uranium states (5f,6d,7s) hybridized with the O-2p states. Another significant feature at about 1.5 eV is attributed to the U5f states. The

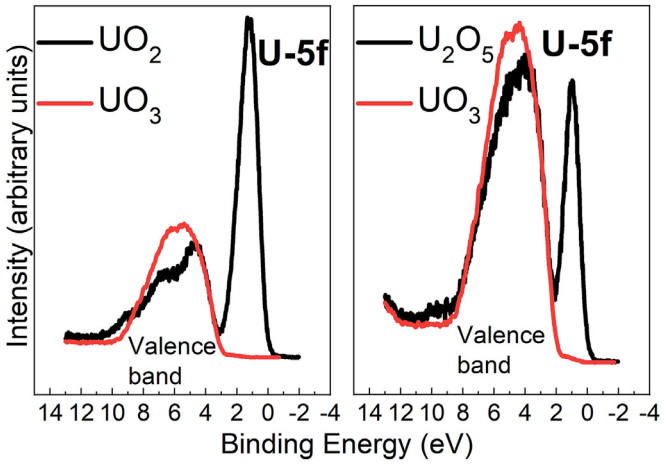

Fig. 1. VB spectra of U_2O_5 (a) and UO_2 (b). The O2p background is simulated by a UO_3 spectrum. The low BE flank is well represented by the UO_3 spectrum.

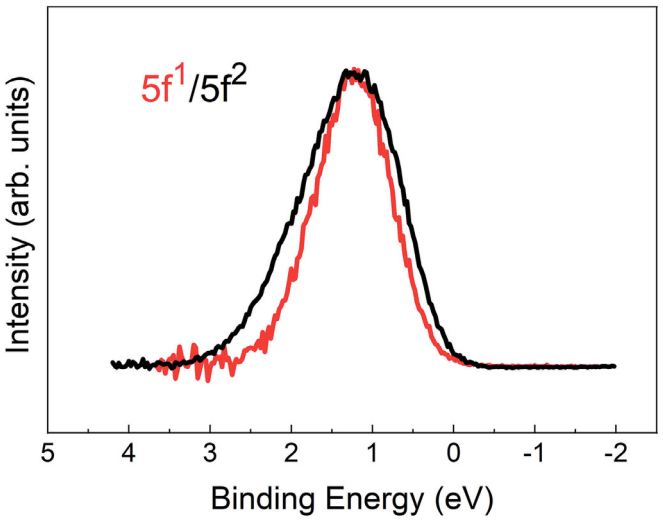

Fig. 2. $5f^1$ and $5f^2$ peaks obtained by subtracting the VB. The shape of $5f^2$ is more asymmetric and broader than $5f^1$.

5f states in uranium oxides are localized, i.e., non-bonding, in contrast to U metal, where they are itinerant and appear as a relatively narrow band pinned at the Fermi-level.

The localized 5f states are shifted away from the Fermi-level E_F to about 1–2 eV binding energy [11]. For the quantification of the 5f occupancy other contributions in the respective spectral range have to be subtracted first, which is crucial especially at low 5f occupancies. In such case the emission at higher binding energy can shift and distort the 5f signal.

Such subtraction is naturally not possible as details of the VB shape are not known. The shape depends on the particular density of states and not simply on the Gaussian-Lorentzian line shapes, as for the core-levels. We therefore use tentatively a numerical subtraction method. The valence-band spectrum of UO_3 (Fig. 1, red spectrum) has no U5f contribution and can be used as a reference state for the other uranium oxides when subtracting the VB spectrum. We assume that the intensity at the pseudogap minimum (i.e., the intensity minimum at about 2 eV) is equally attributed to the VB and the 5f emission. The subtraction then leaves a background that can be attributed to the inelastic electrons (Shirley type) [11]. The subtraction works remarkably well to eliminate the low binding energy part (the falling flank) of the VB, which is in direct proximity to the U5f feature. The high BE part of the VB (around 5–8 eV) is less well reproduced, because the shape of the UO_3 VB is rather different from that for the lower oxidation states. Fortunately, we can neglect this part because it is far away from the U5f line. In addition, the difference of the overall VB shape is less pronounced for U_2O_5-UO_3 then for UO_2-UO_3, because the oxidation states are closer to each other. For the high oxidation state like U_2O_5, the 5f signal is small and close to the VB (Fig. 1b). For the low oxidation state like UO_2 (Fig. 1a), where the VB shapes are less similar, the VB is small compared to the U5f feature, so that only little subtraction is needed and any error by non-perfect subtraction stays small. The resulting spectra of the U-5f emission after VB removal are shown in Fig. 2.

3.2. U5f intensity analysis using the U4f core-level reference

After removal of the VB contribution, the intensity of the U5f line can be reliably quantified. The U5f intensity is directly related to the oxidation state of uranium since the number of 5f states decreases upon oxidation (U(IV) (UO_2): $5f^2$, U(V) (U_2O_5): $5f^1$, U(VI) (UO_3): $5f^0$). The 5f level is localized, without significant hybridization with other uranium states. It is an outer core level. This fact has two important consequences. First, the 5f level has an integral occupation (0,1,2), related to the oxidation state (We neglect intermediate valence which is not observed for simple uranium oxides). Second, the cross-section (σ) of the 5f emission does not vary for the different oxidation states, because it is determined by its orbital character which does not change with oxidation state. This analysis neglects the possibility of differential losses to shake satellites which is outside the scope to this paper.

The photoemission intensity (I) also depends on other parameters, such as spectrometer settings (pass energy, slit size, etc.), inelastic mean free path, etc. [12]. which can all be summarized in one gross intensity parameter (P), which depends on the photoemission line but remains constant for different materials. One may therefore write

$$\boldsymbol{I = P \times I_{h\nu} \times n \times \sigma \times [U]} \quad (1)$$

where P is the intensity parameter, I_{hv} is the X-ray intensity, n is the number of electrons and [U] is the concentration of uranium. I_{hv} and [U] can be eliminated by using a reference line, in our case the U4f line. The U5f/U4f intensity ratio can be expressed as:

$$\frac{\boldsymbol{I_{U5f}}}{\boldsymbol{I_{U4f}}} = \frac{\boldsymbol{P_{U5f}}}{\boldsymbol{P_{U4f}}} \times \frac{\boldsymbol{n_{U5f}}}{\boldsymbol{n_{U4f}}} \times \frac{\boldsymbol{\sigma_{U5f}}}{\boldsymbol{\sigma_{U4f}}} \quad (2)$$

all remaining parameters except n_{5f} are constant. They can be expressed by one variable (c) and the only parameter left is n_{U5f}.

$$\frac{\boldsymbol{I_{U5f}}}{\boldsymbol{I_{U4f}}} = \boldsymbol{c} \times \boldsymbol{n_{U5f}} \Rightarrow \boldsymbol{n_{U5f}} = \frac{1}{\boldsymbol{c}} \times \frac{\boldsymbol{I_{U5f}}}{\boldsymbol{I_{U4f}}} \quad (3)$$

c is evaluated by calibrating to a material of known composition, e.g. UO_2, where n_{5f}=2. In this way we have a simple method to determine the U5f count directly from the intensity of the 5f photoemission line. For simple uranium oxides, the oxygen composition (x) and formal uranium oxidation state (n) of $U^{n+}O_x$ is related to n_{5f} by

$$\boldsymbol{x} = 3 - \boldsymbol{n_{5f}}/2 \quad (4)$$

$$\boldsymbol{n} = 2\,\boldsymbol{x} \quad (5)$$

We assume that the films are homogeneous and, as a consequence, the different escape depths of the U4f and U5f lines have no influence. This is a valid assumption since we work on thin films (<20 nm) and at high temperature (400 °C), where the diffusion, making the films homogeneous, is fast. Also absence of impurity overlayers, which would attenuate the U4f and U5f lines differently, was checked by XPS.

3.3. The U5f shape

The U5f photoemission peak contains an unresolved multiplet structure, which depends on the 5f count (n_{5f}). Multiplets are commonly observed in open-shell systems with partially filled localized outer states. They occur in core-level emissions due to the exchange interaction of the core hole with the open shell [13], but they also occur in photoemission from the open shell themselves (4f in lanthanides, 5f in actinides, or isolated atoms – e.g. gaseous lead [14]). Multiplets have been extensively used to discuss the 4f (open shell) spectra of the rare earth compounds where they correctly account for the often complex 4f spectra [15]. Within the actinide series, 5f multiplet structures are commonly observed in systems with localized 5f electrons, e.g. Am [16] and Cm [17]. We therefore apply a similar analysis to the U oxides, which also have localized 5f states. U(IV) has two f electrons ($5f^2$), and after excitation of a photoelectron the $5f^1$ final state is obtained, which has a multiplet structure [18]. The multiplet terms are broadened by phonon excitations and lifetime effects, eventually resulting in an asymmetric line, as shown in Fig. 2. U(V) has a $5f^1$ initial state configuration which, after emission of the photoelectron, leads to the $5f^0$ final state, which is closed shell and therefore has no multiplet structure. The peak appears as a singlet, which is symmetric and narrower than the $5f^2$ peak (Fig. 2). The exact origin of the multiplets, which involve also correlation effects, as manifested trough configuration interaction [14], is beyond the scope of this paper.

The 5f shape is thus an intrinsic property revealing the oxidation state of U. Pure U(IV) will have a $5f^2$ emission ($5f^1$ final state) and pure U(V) will have a $5f^1$ emission ($5f^0$ final state). In case of mixed oxides (intermediate oxidation states or simply heterogeneous overlayers with concentration gradient between surface and bulk) the 5f emission may be a mixture of $5f^1$ and $5f^2$. A given intensity may well be due to the superposition of $5f^2$ and $5f^0$ states (corresponding to U(IV) and U(VI), respectively), [19] in which case it has a pure $5f^2$ shape (broad), because only U5f^2 gives a signal. But the same intensity could be produced by a pure $5f^1$, in which case it appears as a narrow symmetrical $5f^1$ singlet. This feature is very useful when identifying whether UO_2 surface oxidation proceeds directly to U(VI) or whether U(V) is formed as an intermediate. Similar information can be obtained by analysis of the U4f shake up satellite. The U(VI), U(V) and U(IV) satellites are separated from the main line by 9.7, 7.9 and 6.9 eV, respectively. [8,9,20] Ilton et al. [21] used also the U5d core level peaks to determine the oxidation states and showed its higher sensitivity to oxidation induced changes of uranium. In this analysis we relate the oxidation state to the nominal 5f occupation, neglecting the covalent character of the U-O bond, which has been shown to be weak [22].

3.4. Characterization of the pure oxides: UO_2, U_2O_5 and UO_3

By applying the intensity analysis to uranium oxides of known composition (Fig. 3), an initial calibration of the method is performed. In our experiment the reference compounds are synthesized in-situ from an initial UO_{2+x} (x<0.1) film, produced by sputter deposition. It must be ascertained that their composition is correct. For UO_2 this is simple because it is the lowest possible pure oxide. It is obtained by exposing any higher uranium oxide to atomic hydrogen, which stops reducing once stoichiometric UO_2 is reached. In addition, any further decrease in oxygen concentration (induced e.g., by sputter cleaning stoichiometric UO_2), leads to the appearance of metallic uranium, [23] which has a U4f photoemission line very different from UO_2 and thus easily detectable.

UO_3 synthesis is also straightforward because it is the highest possible uranium oxide. It can be generated by exposing any U oxide to a saturation dosage of atomic oxygen. U_2O_5 is more difficult to produce since it is an intermediate oxide between UO_2 and UO_3.

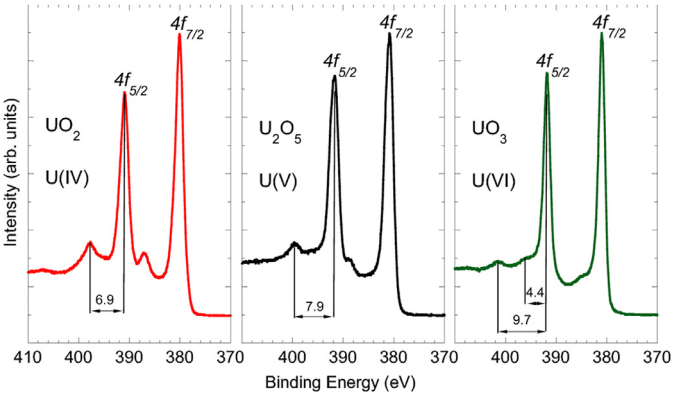

Fig. 3. U4f spectra of UO_2, U_2O_5 and UO_3.

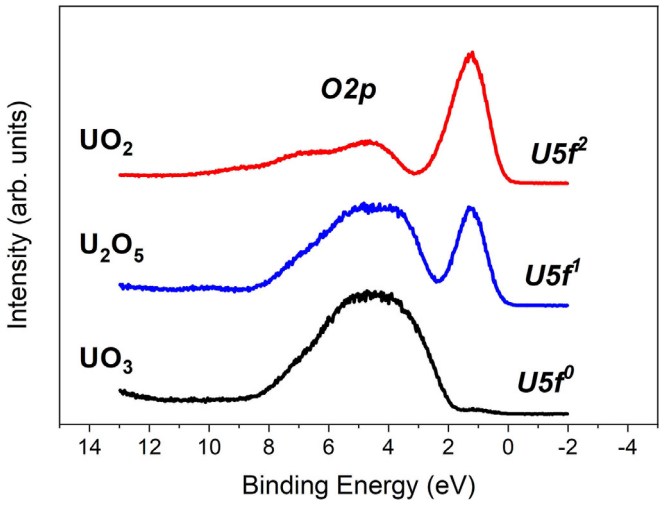

Fig. 4. Valence region spectra for UO_2, U_2O_5 and UO_3.

In general, U(V) is not obtained as a pure state but rather in mixed oxides U_4O_9, U_3O_8, etc. where uranium is present in two oxidation states (e.g., U_4O_9 contains 50% U(IV) and 50% U(V)).

We have previously succeeded in producing nearly pure U(V) by reducing UO_3 with an appropriate dosage of atomic hydrogen. [24] As a criterion for correct composition, we used the U4f satellite which is characteristic for U_2O_5 (ΔE = 7.9 eV), and different from the UO_3 and UO_2 satellites (ΔE = 9.7 and 6.7 eV) (Fig. 3). The increasing energy separation between the satellite and the main line with increasing oxidation state has been discussed by Bagus. [25] Also, the BE of the main peak can be used to determine the valence state. With increasing oxidation state, the 4f shifts to higher BE. However, the BE not only depends on the oxidation state, but also on other factors such as the work function or Fermi-energy, which easily change when the sample is oxidized or adsorbs atoms or molecules (e.g., O, H_2O).

The valence spectra of the three single oxidation state oxides are shown in Fig. 4. UO_2 has a broad intense 5f emission. Upon oxidation, the 5f peak decreases in intensity and narrows, reflecting the evolution from the $5f^2$ doublet to the $5f^1$ singlet. The strong decrease in intensity compared to the O2p VB is due to the simultaneous decrease of the U-5f and increase of the O2p intensities. This illustrates the necessity of using core level reference data when quantifying the intensity changes.

The evolution of the U5f/U4f intensity ratios is shown in Fig. 5. The ratio decreases almost linearly with increasing oxidation state, confirming the above statement, that the ratio only depends on the 5f counts (n_{5f}). This simple relationship allows deduction of the av-

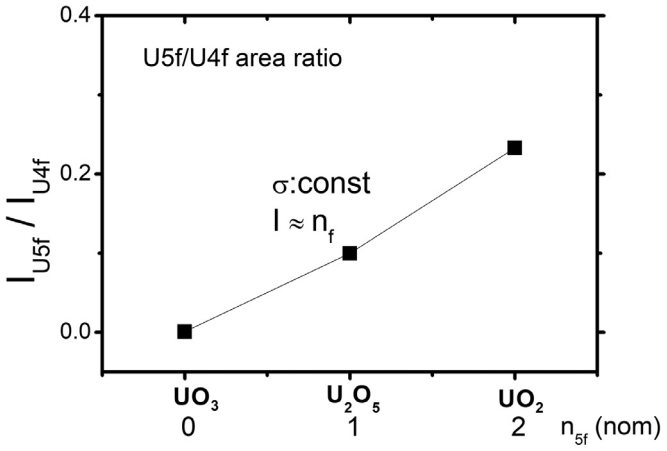

Fig. 5. Evolution of the U5f/U4f intensity ratios for the three pure oxides.

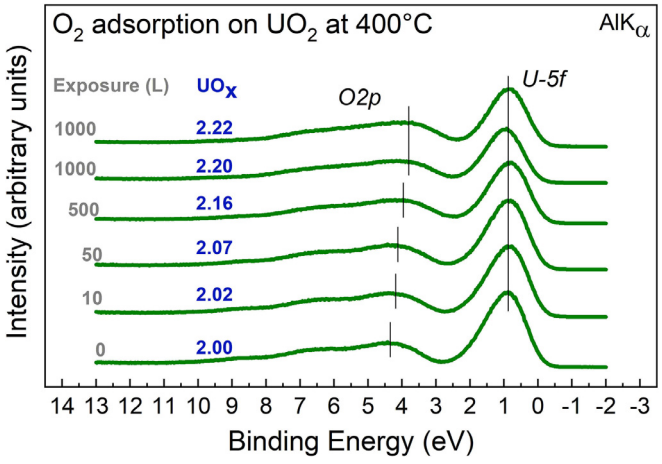

Fig. 6. Reaction of UO_2 with molecular oxygen at 400 °C. Valence region spectra.

erage oxidation state of an unknown (non stoichiometric) uranium oxide from the U5f/U4f intensity ratio. The $U5f^1$ intensity of nominal U_2O_5 displays a certain experimental uncertainty, because it is difficult to produce pure stoichiometric U_2O_5 (there are easily slight admixtures of U(IV) or U(VI)). However, the $U5f^2$ signal of UO_2 is stable, and because a linear relationship exists between the U5f/U4f intensity ratio and n_{U5f}, n_{U5f} of non-stoichiometric compounds (UO_x) can be determined. It represents an average value over the region probed by XPS, which is about 7 monolayers deep.

3.5. Exposure of UO_2 to molecular oxygen

When UO_2 is exposed to molecular oxygen in water as well as under UHV conditions it is oxidized to UO_{2+x} [9,26]. Under UHV conditions, O_2 adsorbs and dissociates to atomic oxygen on UO_2. The atomic oxygen can become incorporated into the lattice and thereby oxidize UO_2. We have performed a study where thin UO_2 films (20 nm) were exposed to molecular oxygen at 400 °C.

We applied the U5f/U4f intensity analysis to determine the surface average oxidation state of surface U.

The series of exposures shows a decrease in U5f intensity with increasing oxygen exposure for moderate exposures. At higher exposures, the intensity changes very little with increasing exposure. The surface composition deduced from the U5f/U4f intensity ratio is indicated in Fig. 6. The composition is averaged over the XPS information depth of about 7 monolayers. Above about 1560 L O_2 dosage, oxidation does not proceed any further than to $UO_{2.22}$.

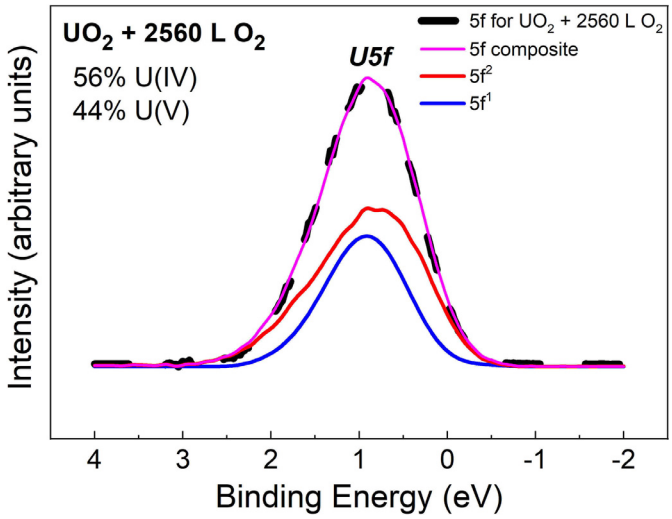

Fig. 7. Decomposition of 5f (after 2560 L O_2) into the $5f^1$ and $5f^2$ components. The $5f^2$ has been subtracted from the sum spectrum.

The 5f peak narrows upon surface oxidation. The initial peak had a pure $5f^2$ shape, typical for UO_2. After exposure to 2560 L O_2, the 5f peak is best reproduced by a mixture of 44% $U5f^1$ and 56% $5f^2$ (Fig. 7). This corresponds to a surface composition of $UO_{2.22}$. The $5f^1$ peak lies in the envelope of the $5f^2$ peak. Upon oxidation, the $5f^2$ peak is gradually replaced by the $5f^1$ peak. This leads to a narrowing of the overall peak.

Analysis of the 5f intensity and shape allows quantification of uranium oxidation upon oxygen incorporation into the films. These methods can be compared to core level analysis giving similar information. In total, there are three independent methods to determine the film oxygen composition and U oxidation state. 1) The U5f/U4f intensity ratio gives the amount of U(IV) and U(V). The oxygen concentration in UO_{2+x} is obtained by $x = 0.5^*[U(V)]$, under the assumption that there is no U(VI).

2) The decomposition of the U4f line into a U(IV) and U(V) component, is done by numerically subtracting the UO_2 spectrum from the composite spectrum. The U4f spectrum only shows U(IV) and U(V) contributions . No U(VI) main line is observed. This interpretation is corroborated by the U4f shake up satellites, which show only U(IV) and U(V) but no U(VI). 3) The O1s/U4f intensity ratio, normalised to the ratio for UO_2 directly yields the total oxygen concentration. Results are compared in Fig. 8. The final film composition averaged over the three methods is $UO_{2.25\pm0.045}$. This composition is close to $UO_{2.2}$, given by the width of the U-5f emission (Fig. 7). At this composition, oxidation does not proceed any further. We attribute this to the accumulation of oxygen at the top surface, where all U(IV) would be transformed into U(V). XPS, with its information depth of 7 monolayers, shows a lower oxygen concentration as it also probes the reduced subsurface.

3.6. Exposure of UO_2 to atomic oxygen

Atomic oxygen oxidizes UO_2 to UO_3, Fig. 9, at sufficiently high dosage [10]. For full conversion, the exposure must be performed at elevated temperature (400 °C) to allow oxygen to diffuse into the deeper layers. At room temperature, some residual UO_2 signal is always left, even at high dosages of atomic oxygen. It is observed both for the U4f, where the U(IV) main peak with its characteristic satellite ($\Delta E = 6.9$ eV) is preserved, and for the valence region spectra, where the U5f peak is seen (it is absent for f^0 of U(VI)).

Here we present data for UO_2 films exposed to low dosages (short exposure times) of atomic oxygen at elevated temperature.

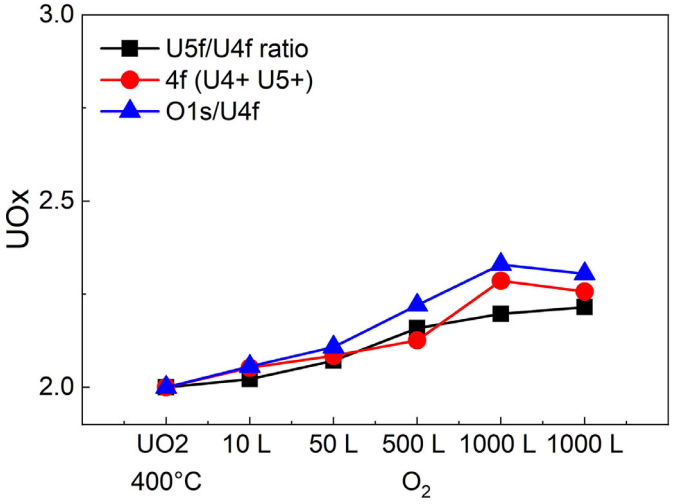

Fig. 8. Film composition by three independent measurements.

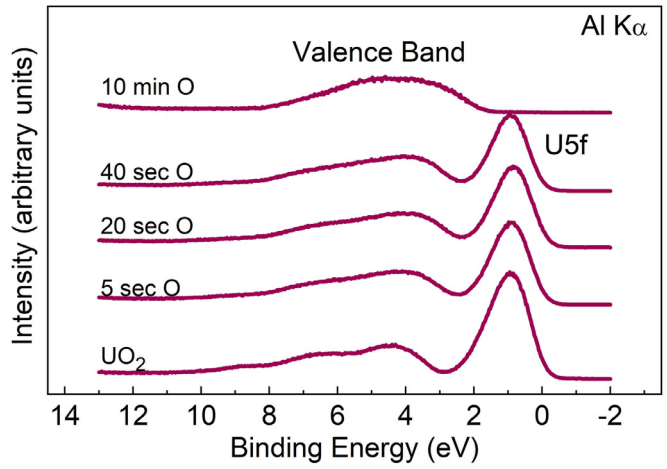

Fig. 9. Valence region. Atomic oxygen plasma at 400 °C.

Table 1
Oxygen composition of UO_3 films exposed to atomic oxygen, determined by analysis of I) I(U5f)/I(U4f), II) I(U4f) (U^{IV} U^{V}), and III) I(O1s)/I(/U4f).

Method nb.	U5f/U4f I	U-4f (U^{IV} U^{V}) II	O1s/U4f III
UO_2	3	3	3
5 secs O	2.98	2.96	2.98
20 secs O	2.91	2.91	2.96
40 secs O	2.86	2.88	2.87

The purpose of low dosage exposure is to catch the initial phase of surface oxidation by atomic oxygen which would otherwise proceed all the way to UO_3. With increasing O dosage, the intensity of the 5f emission decreases and the peak narrows. Narrowing is due to the replacement of the $5f^2$ by the $5f^1$. This is illustrated for the spectrum after 20 secs exposure. The 5f shape is reproduced in Fig. 10 by superposition of $5f^2$ (0.46) and $5f^1$ (0.54). This corresponds to a surface composition of $UO_{2.27}$.

Determination of composition by the 5f analysis can again be compared to the determination by core-level analysis of the oxide shifted U4f components and the O1s/U4f intensity ratios (Table 1). The U5f/U4f ratio gives the lowest value, while the O1s/U4f gives the highest. The U4f spectra show that no U(VI) is formed (absence of U(VI) characteristic main peak and shake up satellite). So only

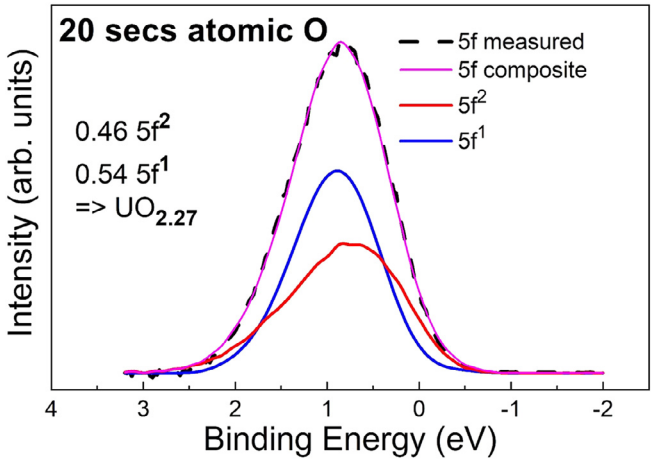

Fig. 10. U5f emission after atomic oxygen exposure.

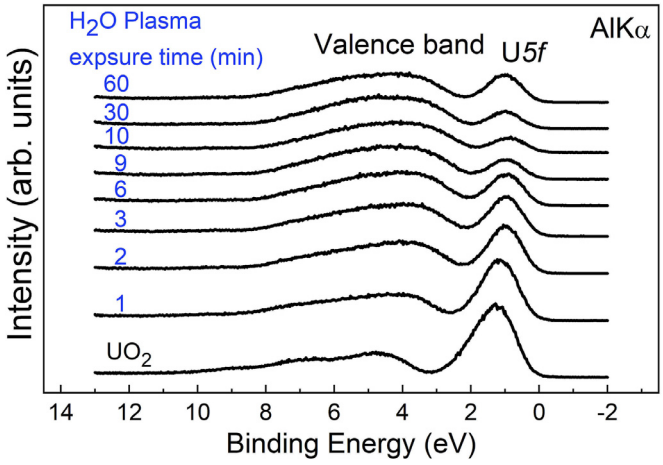

Fig. 11. Valence region spectra of UO_2 films exposed to water plasma.

the U(IV) and U(V) components have to be considered in method 2. The overall agreement between the three methods is very good.

3.7. Exposure of UO_2 to water plasma

Water plasma reacts with the UO_2 surface initially through rapid oxidation. [10] This is attributed to the oxidizing species formed by water dissociation in the plasma (O, $OH^{\bullet}$). Also reducing species are formed in the plasma ($H^{\bullet}$ and H_2), but in the early phase of reaction, oxidation prevails since the surface is in its lowest oxidation state. Studies of UO_2 films exposed to water plasma have been published recently. Here, Fig. 11, we briefly recall the results to apply the U5f analysis. At low water plasma dosage (i.e., for shorter exposure time), up to 10 min, the U5f intensity decreases. This is attributed to UO_2 oxidation to U(V) and U(VI). At high water dosages (exposure times beyond 10 min), U(VI) is again partially reduced to U(V). The U5f signal grows again and the film ends up as a mixture of U(V)/U(VI) at a ratio corresponding to U_3O_8.

Inspection of the U5f peak shape (Fig. 12) reveals that its linewidth very rapidly decreases from the initial $U5f^2$ value and already after 1 min plasma exposure reaches a final value typical for $5f^1$. It then remains constant and only the intensity decreases as U(V) is transformed into U(VI). It will be shown below that some U(IV) is left, but the fraction is so small that it does not influence the linewidth of the U5f. Obviously, the water plasma quickly transforms the UO_2 surface into a mixture of U(V) and U(VI).

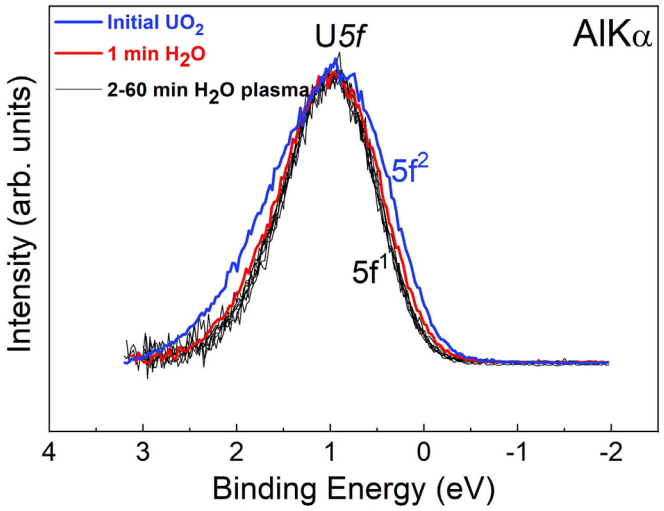

Fig. 12. Evolution of the 5f line width with water plasma exposure.

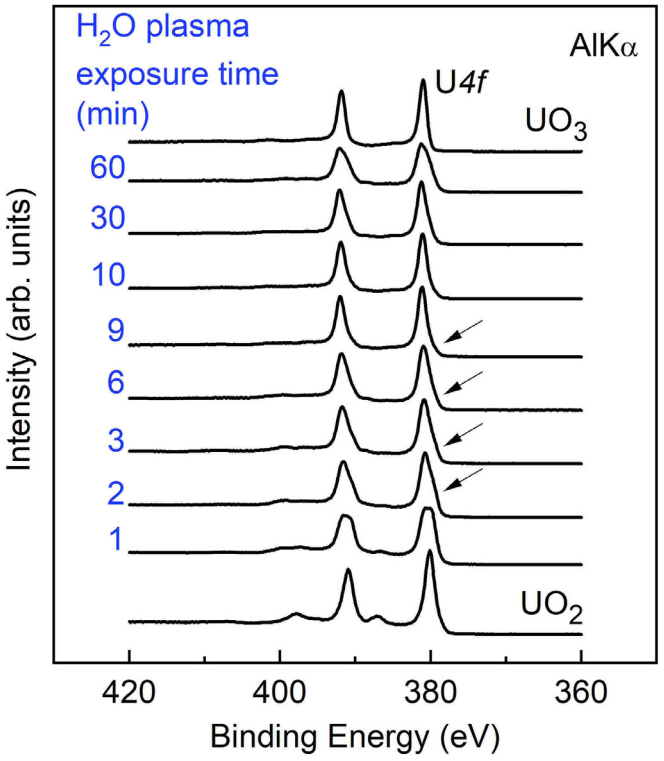

Fig. 13. U4f evolution after water exposure.

All three oxidation states of uranium are present at some stage in the UO_2-water plasma reaction. They are clearly distinguishable by the U4f spectra (Fig. 13). In the early phase (below 10 min exposure) the U(IV) signal persists (arrows in Fig. 13), even though it virtually disappears from the valence region spectra. The U(IV) component is relatively well separated from the U(V) component. Its intensity decreases rapidly but still remains detectable up to 9 min exposure. This is remarkable, considering the very rapid initial oxidation of UO_2 by the water plasma. The UO_2 signal either comes from deeper layers not reached by the oxidation at low dosages, or it is due to some UO_2 left at the surface. For exposures longer than 10 min, U(IV) completely disappears. This coincides with the end of further surface oxidation: at this stage the surface reaches its maximum oxidation state. Comparison with

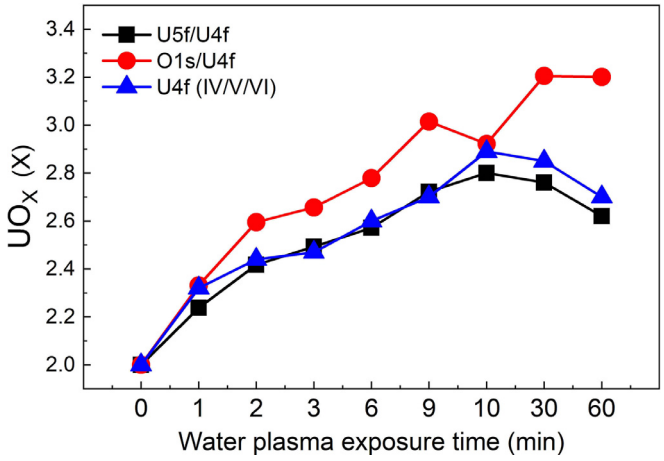

Fig. 14. Oxygen composition of UO_2 films exposed to water plasma, determined by analysis of I) I(U5f)/I(U4f), II) I(U4f) (U^{IV} U^{V}), and III) I(O1s)/I(/U4f).

pure UO_3 shows that at 10 min, the surface is closest to UO_3. The U4f lines are narrow, with the U(VI) component dominating, but at longer exposure times they broaden again indicating that U(VI) is reduced back to U(V). As discussed above the growing U-5f intensity (Fig. 11) confirms that U(V) is formed.

We can now compare the surface compositions of UO_2 films exposed to the water plasma as determined by the three intensity methods, Fig. 14.

The U5f/U4f ratio (method 1) shows an increase in oxidation state, with a maximum around 10 min and then a decrease. The U4f lines (method 2) show that all three oxidation states are present at some point. At low dosage U(IV) and U(V) are observed, then U(VI) appears while U(IV) disappears. Separation and integration are done by first subtracting the U(IV) contribution (using a UO_2 spectrum) and integrating it, for exposure times till 9 min. Then the U(VI) contribution is subtracted and integrated. The remaining U(V) spectrum is then integrated.

For exposures up to 10 min the U4f and VB data are remarkably similar. This corresponds to the early phase of water plasma interaction. In this stage the surface has a large fraction of U(IV) which immediately reacts with the plasma (Fig. 12) and is oxidized to U(V). With ongoing surface oxidation, almost all UO_2 disappears. U(VI) formation slows down and the concentration reaches a maximum, while there is still U(V) left. This is depicted both by the U5f/U4f and by the U4f data (Fig. 14). At 10 min, the highest degree of surface oxidation is reached – with a surface composition around $UO_{2.6}$ to $UO_{2.8}$. From here on, the 5f/4f ratio shows a slightly lower oxygen concentration than the U4f (IV/V/VI). The surface composition is higher than $UO_{2.5}$ (i.e. U(V)). After longer water exposure, beyond 10 min, the surface becomes reduced again. The U5f/4f and U4f methods both show U(V) to be formed.

In spite of the fact that the surface is reduced at longer exposures, the O1s/U4f intensity ratio keeps increasing (method 3) and it definitely deviates from the two other measurements. Oxygen must be present in another form. In the long exposures studies [15] we mentioned the formation of a second form of U(V). The O1s peak after 60 min water plasma exposure is broader than after 10 min. However, the O1s of UO_3 (mainly present at 10 min) is broader than the O1s of U_2O_5 (mainly present at 60 min). The further broadening in spite of reduction indicates the presence of a second oxygen species. Subtraction spectrum reveals an intensity increase at around 1.8 eV higher BE than the oxidic peak. The valence region spectra show a small peak at 9.4 eV, which was also seen in UPS. This peak could be attributed to OH. It is small but XPS has a low cross-section for O2p. As described above the pres-

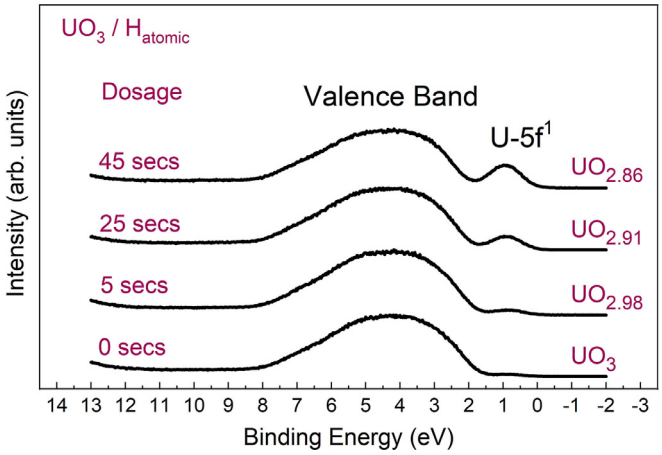

Fig. 15. Valence spectra of UO_3 exposed to /H.

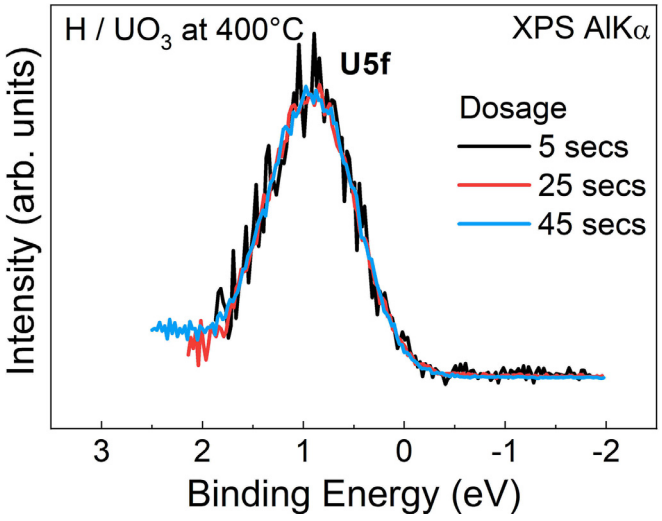

Fig. 16. U5f emission in UO_3 exposed to H.

ence of OH could explain the broadening of the O1s in spite of the U reduction.

3.8. Exposure of UO_3 to atomic hydrogen

Molecular hydrogen does not react with UO_3 at 400 °C, within the typical UHV dosage ranges (below 10^4 L). This is partly due to the weak adsorption on oxidic surfaces and the fact that H_2 is unreactive. H_2 is a small, non-polar molecule. Also, it does not polarize easily. Therefore, it has very low affinity for polar surfaces. Atomic hydrogen, on the other hand, adsorbs more easily. It can directly bind to surface oxygen, which on many oxides forms the topmost layer [27]. Fig. 15 shows the valence region of UO_3 exposed to small dosages of atomic hydrogen. The U5f emission increases steadily with H dosage (exposure time). This shows the surface to be reduced. Its shape does not change (Fig. 16) and stays narrow, which is typical for $5f^1$. Initial reduction of UO_3 leads exclusively to U(V) formation. This has been noticed previously when studying the interaction of mixed water-hydrogen plasma with UO_3, which showed a higher reactivity for reduction of UO_3 than U_2O_5. U_2O_5 is easier to form by reduction than to reduce further.

The surface composition, as determined by the three intensity analysis methods is shown in the table 2. All three methods yield similar values, showing reduction of UO_3. For the 5 secs exposure, method II reaches its limits, because the difference spectrum becomes very small. But the result is still in agreement with the two other methods.

Table 2
Oxygen composition of UO_3 films exposed to atomic Hydrogen, determined by analysis of I) I(U5f)/I(U4f), II) I(U4f) (U^V U^{VI}), and III) I(O1s)/I(/U4f).

Ratio Method number	U5f/U4f I	U4f (U^V/U^{VI}) II	O1s/U4f III
UO_3	3	3	3
5 secs H	2.98	2.96	2.98
20 secs H	2.91	2.91	2.96
45 secs H	2.86	2.88	2.87

After 45 secs exposure, the U(V) satellite appears in the U4f spectrum, which is consistent with the $U5f^1$ emission of U(V) in the valence region. There is no indication for surface OH. Valence band difference spectra do not display any intensity around 10 eV, the position of the OH lines. Also the O-1 s spectrum does not broaden. On the contrary, it narrows as consequence of the surface reduction (U_2O_5 has a narrower O-1 s line than UO_3). It is surprising that after H exposure there is no OH formation, while after long term water exposure there was. The only effect of H exposure is reduction of the UO_3, which in this early phase, forms exclusively U(V).

Conclusion

Analysis of the U5f lines allows determination of the surface oxidation state of binary uranium oxides. After normalization to the U4f, the U5f intensity is proportional to the 5f count (n_{5f}), which in turn is related to the oxidation state of uranium (U(IV) (UO_2): n_{5f}=2, U(V) (U_2O_5): n_{5f}=1, U(VI) (UO_3): n_{5f}=0). Also, the shape of the 5f emission depends on the 5f count and provides a quite simple and straightforward way to deduce the oxidation state of uranium (U(V) and U(IV)) from the corresponding $5f^1$ and $5f^2$ electron configurations. The results of the 5f analysis have been compared to the U4f analysis, which also provides the uranium oxidation state, by the characteristic U4f binding energies and the U4f satellites. Finally, the O1s/U4f intensity ratio gives information on the total oxygen content, which has to be compatible with the distribution of the different oxidation states. The analysis was applied to different oxidation/reduction reactions of the oxide surface: UO_2 reaction with atomic and molecular oxygen and with water plasma, UO_3 reaction with atomic hydrogen. Comparison reveals a very good agreement between the different methods. The analysis showed that oxidation of U(IV) proceeds exclusively via U(V) formation, no trace of U(VI) is found in the early oxidation phase. Vice versa, early reduction of U(VI) proceeds exclusively via U(V), and no U(IV) is found.

Declaration of Competing Interest

There are no conflicts to declare.

CRediT authorship contribution statement

Ghada El Jamal: Investigation, Writing – original draft. **Thomas Gouder:** Investigation, Visualization, Writing – original draft, Writing – review & editing. **Rachel Eloirdi:** Project administration, Resources, Writing – review & editing. **Mats Jonsson:** Supervision, Writing – review & editing.

Acknowledgments

The Swedish Nuclear and Fuel Waste Management Company (SKB) is gratefully acknowledged for financial support. This work

has been partially supported by the ENEN+ project that has received funding from the Euratom research and training Work Programme 2016–2017 – 1#755576. We thank Frank Huber for technical assistance.

References

[1] A.S. Kertes, R. Guillaumont, Solubility of UO2. A comparative review, Nucl. Chem. Waste Manag. 5 (3) (1985) 215–219.
[2] D.W. Shoesmith, Fuel corrosion processes under waste disposal conditions, J. Nucl. Mater. 282 (1) (2000) 1–31.
[3] I. Grenthe, D. Ferri, F. Salvatore, G. Riccio, Studies on metal carbonate equilibria. Part 10. A solubility study of the complex formation in the uranium(VI)–water–carbon dioxide (g)</number>system at 25°C, J. Chem. Soc. Dalton Trans. (11) (1984) 2439–2443.
[4] M.M. Hossain, E. Ekeroth, M. Jonsson, Effects of HCO3- on the kinetics of UO2 oxidation by H2O2, J. Nucl. Mater. 358 (2) (2006) 202–208.
[5] E. Ekeroth, M. Jonsson, Oxidation of UO2 by radiolytic oxidants, J. Nucl. Mater. 322 (2) (2003) 242–248.
[6] M.E. Broczkowski, J.J. Noël, D.W. Shoesmith, The inhibiting effects of hydrogen on the corrosion of uranium dioxide under nuclear waste disposal conditions, J. Nucl. Mater. 346 (1) (2005) 16–23.
[7] S. Sunder, D.W. Shoesmith, M.G. Bailey, F.W. Stanchell, N.S. McIntyre, Anodic oxidation of UO2: part I. Electrochemical and X-ray photoelectron spectroscopic studies in neutral solutions, J. Electroanal. Chem. Interfac. Electrochem. 130 (1981) 163–179.
[8] E.S. Ilton, P.S. Bagus, XPS determination of uranium oxidation states, Surface and Interface Analysis 43 (13) (2011) 1549–1560.
[9] H. Idriss, Surface reactions of uranium oxide powder, thin films and single crystals, Surf. Sci. Rep. 65 (3) (2010) 67–109.
[10] G. El Jamal, T. Gouder, R. Eloirdi, M. Jonsson, X-Ray and ultraviolet photoelectron spectroscopy studies of Uranium(iv), (v)</number> and(vi) exposed to H2O-plasma under UHV conditions, Dalton Trans. 50 (2) (2021) 729–738.
[11] J.R. Naegele, J. Ghijsen, L. Manes, Localization and hybridization of 5f states in the metallic and ionic bond as investigated by photoelectron spectroscopy, Actinides—Chem. Phys.Properties (1985) 197–262.
[12] D. Briggs, M.P. Seah, Practical Surface Analysis: by Auger and X-ray Photoelectron Spectroscopy, Chichester: Wiley, Chichester, 1983.
[13] P. Bagus, C. Nelin, Y. Al-salik, E. Ilton, H. Idriss, Core level Multiplet splitting for the XPS of heavy elements: dependence on oxidation state, Surface Sci 643 (2016) 142–149.
[14] S. Süzer, M.S. Banna, D.A. Shirley, Relativistic and correlation effects in the 21.2-eV photoemission spectrum of atomic lead, J. Chem. Phys. 63 (1975) 3473–3477.
[15] M. Campagna, G.K. Wertheim, Y. Baer, Unfilled inner shells: rare earths and their compounds, photoemission in solid II edts, in: L. Ley, M. Cardona (Eds.), Topics in Applied physics, Springer-Berlin, Heidelberg New York, 1979, pp. 217–260.
[16] J.R. Naegele, M. Manes, J.C. Spirlet, W. Müller, Localization of 5f Electrons in Americium: a Photoemission Study, Phys, Rev. Lett 52 (20) (1984) 1834–1837.
[17] T. Gouder, G. van der Laan, A.B. Shick, R.G. Haire, R. Caciuffo, Electronic structure of elemental curium studied by photoemission, Phys. Rev. B 83 (2011) 125111 1-6.
[18] Y. Baer, Electron Spectroscopy Studies, in: A.J. Freeman, G.H. Lander (Eds.), Handbook on the Physics and Chemistry of the Actinides, North-Holland, Amsterdam Oxford, 1984, pp. 271–339. eds..
[19] K.O. Kvashnina, S.M. Butorin, P. Martin, P. Glatzel, Chemical state of complex uranium oxides, Phys. Rev. Lett. 111 (25) (2013) 253002.
[20] G. El Jamal, T. Gouder, R. Eloirdi, M. Jonsson, Time-dependent surface modification of uranium oxides exposed to water plasma, Dalton Trans. 50 (14) (2021) 4796–4804.
[21] E.S. Ilton, Y. Du, J.E. Stubbs, P.J. Eng, A.M. Chaka, J.R. Bargar, C.J. Neline, P.S. Bagus, Phys. Chem. Chem. Phys. 19 (2017) 30473–30480.
[22] K.I. Maslakov, Y.A. Teterin, M.V. Ryzhkov, A.J. Popel, A.Y. Teterin, K.E. Ivanov, S.N. kalmykov, V.G. Petrov, I. Farnan, The nature of the chemical bond in UO2, Int. J. Quantum Chem. (2019), doi:10.1002/qua.26040.
[23] S.D. Senanayake, H. Idriss, Water reactions over stoichiometric and reduced UO2(111) single crystal surfaces, Surf. Sci. 563 (1) (2004) 135–144.
[24] T. Gouder, R. Eloirdi, R. Caciuffo, Direct observation of pure pentavalent uranium in U2O5 thin films by high resolution photoemission spectroscopy, Sci. Rep. 8 (1) (2018) 8306.
[25] P.S. Bagus, C.J. Nelin, E.S. Ilton, Theoretical modeling of the uranium 4f XPS for U(VI) and U(IV) oxides, J. Chem. Phys. 139 (24) (2013) 244704.
[26] M.J. Nicol, C.R.S. Needes, The anodic dissolution of uranium dioxide—I in perchlorate solutions, Electrochim. Acta 20 (8) (1975) 585–589.
[27] P.W. Tasker, The surface properties of uranium dioxide, Surf. Sci. 87 (2) (1979) 315–324.